A Mouse Model for the ΔF508 Allele of Cystic Fibrosis

Bernhardt G. Zeiher,* Ernst Eichwald,§ Joseph Zabner,* Jeffrey J. Smith,‡ Aurita P. Puga,* Paul B. McCray, Jr.,‡ Mario R. Capecchi,‖ Michael J. Welsh,* and Kirk R. Thomas‖

*Howard Hughes Medical Institutes, *Departments of Internal Medicine and ‡Pediatrics, University of Iowa College of Medicine, Iowa City, Iowa 52242; and Howard Hughes Medical Institute, §Department of Pathology and ‖Eccles Institute of Human Genetics, University of Utah College of Medicine, Salt Lake City, Utah 84112*

Abstract

The most common cause of cystic fibrosis is a mutation that deletes phenylalanine 508 in cystic fibrosis transmembrane conductance regulator (CFTR). The ΔF508 protein is misprocessed and degraded rather than traveling to the apical membrane. We used a novel strategy to introduce the ΔF508 mutation into the mouse CFTR gene. Affected epithelia from homozygous ΔF508 mice lacked CFTR in the apical membrane and were Cl^- impermeable. These abnormalities are the same as those observed in patients with ΔF508 and suggest that these mice have the same cellular defect. 40% of homozygous ΔF508 animals survived into adulthood and displayed several abnormalities found in human disease and in CFTR null mice. These animals should provide an excellent model to investigate pathogenesis and to examine therapies directed at correcting the ΔF508 defect. (*J. Clin. Invest.* 1995. 96:2051–2064.) Key words: animal models • Cl^- secretion • cystic fibrosis • gene targeting • Na^+ absorption

Introduction

Cystic fibrosis (CF)[1] is caused by mutations in the gene encoding the cystic fibrosis transmembrane conductance regulator (CFTR), a phosphorylation-regulated Cl^- channel expressed in the apical membrane of epithelia (1, 2). The most common CF mutation is a 3-bp deletion that eliminates phenylalanine 508 (3). The ΔF508 mutation disrupts the biosynthetic processing of CFTR so that the protein is retained in the endoplasmic reticulum and is then degraded (4). As a result, affected epithelia lack CFTR in the apical membrane (5–7) and lack cAMP-stimulated Cl^- permeability (8).

Several groups have disrupted the mouse CFTR gene to create null mutant mice that lack CFTR (9–11) or express greatly reduced amounts of wild-type protein (12). Those animals have some of the phenotypic features of patients with CF and have been used to evaluate gene therapies. However to understand the pathophysiology of disease and to evaluate new therapies, mice that bear the ΔF508 mutation could offer several advantages. Therefore we used a novel targeting strategy to introduce the ΔF508 mutation into the mouse CFTR gene (13). Murine CFTR is 78% identical to human CFTR (14, 15) and it contains a phenylalanine at residue 508 flanked by 28 amino acids identical to those in human CFTR. The goal of this work was to generate animals homozygous for the ΔF508 mutation (ΔF/ΔF mice).

Using these animals, we could determine if the ΔF508 mutation in mouse CFTR leads to a lack of CFTR protein and Cl^- impermeable epithelia, similar to what is found in humans. Answering this question is important because most previous studies of ΔF508 protein have been performed with human CFTR in recombinant systems and it would be very useful to have an in vivo model. We also asked the related question, do ΔF/ΔF mice have a phenotype that resembles CF in humans and is their phenotype similar to that of null mice? On one hand, ΔF/ΔF mice might have minimal disease if the ΔF protein is processed normally in mice and has substantial residual function. On the other hand, ΔF/ΔF mice could have a phenotype similar to null mice if mouse ΔF508 CFTR is misprocessed. Finally, ΔF/ΔF mice might have a more severe phenotype if the ΔF protein conferred some negative effect. This latter possibility seemed unlikely because non-CF humans who carry a ΔF508 mutation on one chromosome are phenotypically normal.

An animal model would also allow us to test new treatments that might correct the ΔF508 processing defect. Such a treatment would be appealing because many patients with CF have this mutation (the ΔF508 allele occurs on ~ 70% of CF chromosomes) (3), because the ΔF508 protein retains partial Cl^- channel activity (16, 17), and because even a small increase in the amount of functional protein at the cell surface may be sufficient to prevent disease (18). We previously showed that the ΔF processing defect could be corrected in vitro by reducing the incubation temperature (16). A ΔF/ΔF mouse would allow an in vivo test of this and other strategies such as those designed to alter the interaction of the mutant protein with chaperones.

Address correspondence to Kirk R. Thomas, Howard Hughes Medical Institute, Eccles Institute of Human Genetics, Research Facility, University of Utah, Salt Lake City, UT 84112. Phone: 801-581-3841; FAX: 801-585-3425.

Received for publication 19 April 1995 and accepted in revised form 27 July 1995.

1. *Abbreviations used in this paper:* CF, cystic fibrosis; CFTR, cystic fibrosis transmembrane conductance regulator; neo^r, neomycin phosphotransferase; I_{sc}, short-circuit current; RT-PCR, reverse transcription-polymerase chain reaction; Vt, transepithelial voltage.

J. Clin. Invest.

0021-9738/95/10/2051/14 $2.00
Volume 96, October 1995, 2051–2064

Methods

Generation of mice. Construction of the targeting vector and identification of ES cells containing either the ΔF allele or the neomycin phosphotransferase (neo^r) allele (see Fig. 1 *A*) have been described (13). The parental ES cell line was CC1.2 (19) derived from mouse strain 129/Sv/Ev, which carries an Agouti (A^w) coat color marker. ES cells heterozygous for the individual mutant CFTR alleles were injected into C57B1/6J blastocysts as described previously (20). Chimeric animals with > 50% Agouti coat color were bred and the DNA of their Agouti progeny assayed by Southern transfer analysis for the presence of the mutant allele (13). Heterozygotes carrying each mutation (either ΔF or neo^r) were backcrossed to C57B1/6J animals to establish the individual colonies. The genetic background of the animals used in this study thus approximates 25%–129/75%-B16.

Animals heterozygous for the ΔF mutation were paired and males removed after 2 wk. Cages were examined daily to monitor the approximate time of birth and to assess mortality. Tissue from dead animals was genotyped by PCR; live animals were genotyped at weaning by analysis of DNA extracted from a tail clip. Genotyping was performed by Southern analysis or by PCR as described (13, 21). Animals had a diet of Teklad 10% Mouse Breeder Diet (Tekclad Premier Laboratory Diets, Madison, WI).

Reverse transcription PCR (RT-PCR). Total RNA was isolated from tissue dissected from individual animals by the guanidinium thiocyanate/LiCl method (22). Tissue that was not immediately processed was quick-frozen in liquid nitrogen and stored at −80° until use. RNA was reversed transcribed by Maloney murine leukemia virus polymerase (GIBCO BRL, Rockville, MD) under published conditions and cDNA was quantitated by PCR using primers homologous to the mouse β-actin gene (23, 24). These results were used to load equal amounts of cDNA in the CFTR amplification reaction. Amplification was performed in either an Air Thermo-Cycler (Idaho Technologies, Inc., Idaho Falls, ID), or a DNA Thermal Cycler (Perkin-Elmer Cetus Corp., Norwalk, CT). Cycle temperatures and times were as follows: 60°, 0 s; 72°, 6 s; 95°, 0 s in the air cycler, and 60°, 6 s; 72°, 12 s; 95°, 6 s in the thermal cycler. Actin cDNA was quantitatively amplified in 13 cycles. CFTR cDNA was identified by amplification between both 9th and 10th exon sequences (205-bp product) and 9th and 11th exon sequences (268-bp product), and 10th and 11th exons (150-bp product). The following primers were used: 9th exon, 5′-CTGGATCTACTGGACTAGGA-3′ (sense strand); 10th exon, 5′-GGCAAGCTTTGACAACACTC-3′ (antisense strand); 10th exon 5′-GGATTATGCCGGGTACTATC (sense strand); 11th exon, 5′-ACTCCACCTTCTCCAAGAAC-3′ (antisense strand). Amplification conditions were similar to that for actin, but the annealing temperature was 58° and the cycle number increased to 26 cycles for the 9th–10th exon amplification and 22 cycles for the 9th–11th exon and 10th–11th exon amplification. All amplifications were performed using GIBCO BRL reagents and in the presence of [^{32}P]dCTP. Amplification products were analyzed by electrophoresis on both native and denaturing 6% acrylamide gels followed by autoradiography. To distinguish wild-type from ΔF transcripts, RT-PCR products were restricted with HindIII. The two products were resolved by virtue of their 3-bp difference on a DNA sequencing gel.

Histology. Animals were killed by cervical dislocation. All tissues were examined at the macroscopic level before fixation in 4% formaldehyde. Fixed tissue was embedded in paraffin, sectioned (6 μm) and stained either by hematoxylin and eosin or by Periodic-acid-Schiff (PAS) according to standard protocols. Stained sections were all examined in a blinded fashion by light microscopy.

Measurement of nasal voltage. The transepithelial electric potential difference (Vt) across the nasal epithelium was measured using techniques similar to those previously described (25, 26). Investigators were blinded to the animal's genotype. Mice were anaesthetized with an intraperitoneal injection of 2,2,2 tribromoethanol (16 μl/gram). A 23-gauge subcutaneous needle connected with normal saline solution to a Ag/AgCl pellet (E.W. Wright, Guilford, CT) was used as a reference electrode. The exploring electrode was a 200-μm flexible catheter filled with a Ringer's solution containing (mM), 135 NaCl, 2.4 KH_2PO_2, 0.6 K_2HPO_4, 1.2 $CaCl_2$, 1.2 $MgCl_2$, and 10 Hepes (titrated to pH 7.4 with NaOH) and connected to a Ag/AgCl pellet. Voltage was measured with a voltmeter (Keithley Instruments Inc., Cleveland, OH) connected to a strip chart recorder (Servocorder; Watanabe Corporation of America, Costa Mesa, CA). The exploring catheter was inserted 4–5 mm into the nostril and the basal Vt was recorded. Once a stable baseline was achieved, Ringer's solution containing 100 μM amiloride (Merck and Co. Inc., West Point, PA) was then perfused through the second catheter at a rate of 50 μl/min using a syringe pump (Sage Instruments, Cambridge, MA). After 5 min, the perfusing solution was changed to a solution containing 135 mM NaGluconate (substituted for NaCl) 10 μM terbutaline, and 100 μM amiloride. Measurements were made after perfusion for 5 min.

Study of intestinal epithelium. Sections of jejunum were excised and mounted in modified Ussing chambers (Jim's Instrument Manufacturing Inc., Iowa City, IA) to measure short-circuit current and transepithelial resistance as previously described (11). Investigators were blinded to the animal's genotype. Tissues were bathed in a symmetrical Ringer's solution containing (mM): 118 NaCl, 20.4 $NaHCO_3$, 2.4 K_2HPO_4, 0.6 KH_2PO_2, 1.2 $CaCl_2$, 1.2 $MgCl_2$, pH 7.4 bubbled with a 95% O_2/5% CO_2. cAMP agonists (10 μM forskolin and 100 μM IBMX) were added to both mucosal and serosal solutions. Bumetanide (100 μM) was added to the serosal surface to inhibit the Cl^- current. If no increase in current was observed with the addition of cAMP agonists, intestinal viability was determined by adding 5 mM dextrose to the mucosal surface followed by inhibition of Na^+-glucose cotransport by addition of 200 μM phloridzin. One +/+, two +/ΔF, and two ΔF/ΔF intestines failed to respond to cAMP agonists and/or to dextrose; they were considered to be nonviable and were excluded from further analysis.

Study of pancreatic duct epithelia. Pancreatic interlobular duct epithelium was isolated and cultured using methods similar to those previously described (27). When the cells had reached 80% confluence (7–14 d), they were trypsinized and seeded onto human placental collagen-coated 12 mm millicells (Millipore Corp., Milford, MA). Once epithelia reached confluence (4–7 d) some were used to study transepithelial electrical properties and others were used to study fluid secretion. Those used for electrophysiology were mounted in modified Ussing chambers and bathed in a symmetric solution of 1:1 DMEm/HAM'S F12, warmed to 37°C, and bubbled with a 95% O_2/5% CO_2 mixture. Short-circuit current (I_{sc}) was recorded continuously and transepithelial resistance was measured as described above. Once a stable baseline was established, cAMP agonists (10 μM forskolin and 100 μM IBMX) were added to the mucosal and submucosal solutions. After 20 min, 2 mM diphenylamine-2-carboxylate was added to the mucosal solution to inhibit Cl^- secretion. If there was no response to cAMP agonists, the viability of epithelia was assessed by adding the Ca^{2+} ionophore A23187 (1 μM to the mucosal surface). One +/+, one +/ΔF, and no ΔF/ΔF epithelia failed to respond to cAMP agonists and/or to A23187; they were considered to be nonviable and were excluded from further analysis.

To measure fluid transport we used techniques similar to those previously described for cultured human airway epithelia (28). Briefly, the submucosal solution of confluent epithelia was replaced with 3.5 ml of fresh serum-supplemented culture media. The mucosal solution was replaced with 100 μl of serum-free media. Monolayers were exposed to either no agonists (basal) or cAMP agonists (10 μM forskolin and 100 μM IBMX) added to mucosal and submucosal solutions. To minimize evaporative loss, the mucosal surface was covered with 140 μl filter-sterilized mineral oil (previously warmed to 37°C, humidified, and equilibrated with 5% CO_2). After 24 h, the mucosal solution was collected in capillary tubes and volume was measured (28). Preliminary experiments revealed that after adding 100 μl of media to the mucosal surface 95.1±0.4 μl (n = 15 millicells) could be recovered 10 min later. This volume served as the zero volume. Net fluid transport represents the volume recovered at 24 h minus 95.1 μl.

Immunocytochemistry. Fresh tissues were excised, fixed in 4% para-

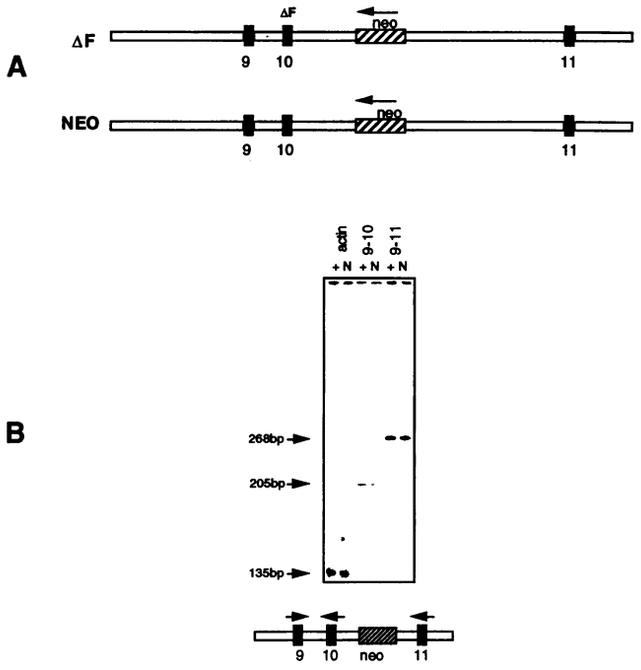

Figure 1. (*A*) Mutant CFTR alleles. The top line represents the ΔF allele. It contains the deletion of 3 coding-strand nucleotides, CTT, corresponding to the human ΔF508 allele, as well as a 3 kb insertion of the neo^r gene in intron 10. Transcription of the neo^r gene is opposite to that of CFTR. The bottom line represents the neo^r allele that contains only the neo^r insertion in intron 10 but is wild type in exon 10. (*B*) Quantitation of CFTR mRNA from wild-type and neo^r alleles. Total RNA was isolated from the upper bowel of wild-type (+) and neo^r/neo^r (N) adult mice. Diagram at bottom shows location of PCR primers.

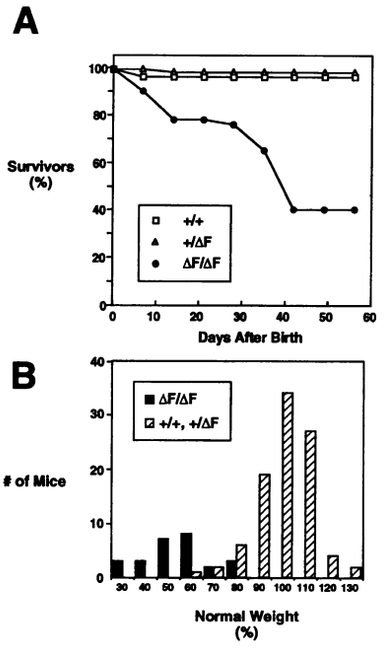

Figure 2. (A) Viability of progeny from a +/ΔF intercross. Weaning occurred at approximately 30 days. n = 34 +/+, 73 +/ΔF, and 41 ΔF/ΔF. (B) Weight distribution of progeny from the +/ΔF intercross. Animals generated as in (A) were genotyped and weighed at weaning (approximately 30 days after birth). To compensate for litter to litter size variation, the mean weight of the +/+ and +/ΔF animals was determined. The weight of individual mice was scored as a percentage of that mean weight. Data are from 95 +/ΔF and +/+ mice and 26 ΔF/ΔF mice.

formaldehyde, cryoprotected in 0.5 M sucrose, and frozen in liquid nitrogen. 6-μm cryosections were permeabilized with 0.2% Triton-X and blocked with Superblock (Pierce, Rockford, IL) for 1 h. A polyclonal antibody (pC-term B; Genzyme Corp., Boston, MA) against the COOH-terminal portion of CFTR was used to localize CFTR. The primary antibody was diluted 1:100 in PBS/1% donkey serum and incubated with sections for 1 h. Sections were then rinsed three times with PBS and incubated with a 1:400 dilution of donkey anti-rabbit-Cy3 (Jackson ImmunoResearch Laboratories, Inc., West Grove, PA) for 30 min. Sections were then rinsed three times with PBS and mounted in Gelmount (Biomeda Corp., Foster City, CA). Specimens were examined on a Leica fluorescent microscope (Leica AG, Heerbrugg, Switzerland). Photomicrographs were obtained using a cooled CCD camera (Optronics Engineering, Goleta, CA) and printed on a color videoprinter (Sony Corp., Tokyo, Japan). Identical exposures were used for normals and controls. Negative controls included no primary antibody, nonimmune rabbit serum, and tissue from mice known to have a disruption in the CFTR gene (11).

Statistical evaluation. For the physiologic data, when more than one data point was available from an individual mouse (for example, two pieces of intestine studied from one mouse), a mean of those values was used for statistical comparison. Data are presented as mean±SEM. A one-way ANOVA was used to compare the three groups. When a significant difference was found by analysis of variance, Bonferonni-adjusted *t* tests were applied to determine which groups were significantly different.

Results

Generation of mutant animals. We introduced a deletion corresponding precisely to the human ΔF508 allele via gene targeting in ES cells (21). ES cells containing the ΔF mutation were selected by virtue of genetic linkage of the ΔF mutation in CFTR exon 10 with a neo^r gene inserted into CFTR intron 10 (13). The mutant allele, depicted at the top of Fig. 1 *A*, thus contained both the ΔF mutation and the neo^r insertion. We anticipated that the *neo^r* gene would have a minimal effect on the expression of the CFTR gene. First, it contained a strong polyadenylation signal to reduce the chance of readthrough transcription into the CFTR gene. Second, it was placed in a transcriptional orientation opposite to that of CFTR gene expression so that the CFTR message would not be prematurely terminated by signals in the *neo^r* gene. Third, the neo^r sequences were located 4 kb downstream of the exon 10 splice donor site and at least 8 kb upstream of the exon 11 splice acceptor site, to minimize any effect on excision of the 10th intron. To verify that the *neo^r* gene would be neutral in terms of CFTR, we also introduced a neo^r allele alone (*bottom line,* Fig. 1 *A*) into ES cells. Two ES cell lines, one containing the ΔF allele (linked to neo^r) and one containing only neo^r, were injected into blastocysts to generate chimeric animals. The chimeric animals were then bred to generate founder animals, heterozygous for the two different CFTR alleles.

The neo^r allele is neutral. To assess any potential impact of the *neo^r* gene in intron 10, we analyzed offspring of mice heterozygous for the neo^r allele (without the ΔF mutation). There was no detectable phenotype: viability and size were the same for wild-type, heterozygous, and homozygous neo^r progeny. Moreover, the neo^r allele was able to completely rescue the overt phenotypes (see below) induced by the ΔF mutation: compound heterozygotes containing one neo^r allele and one ΔF allele were indistinguishable from wild-type animals (not shown). At the transcriptional level the *neo^r* gene had no detectable quantitative or qualitative effect on mRNA transcribed from the CFTR locus. Total RNA was prepared from the small bowel of wild-type animals and mice homozygous for the neo^r allele and subjected to quantitative RT-PCR (23).

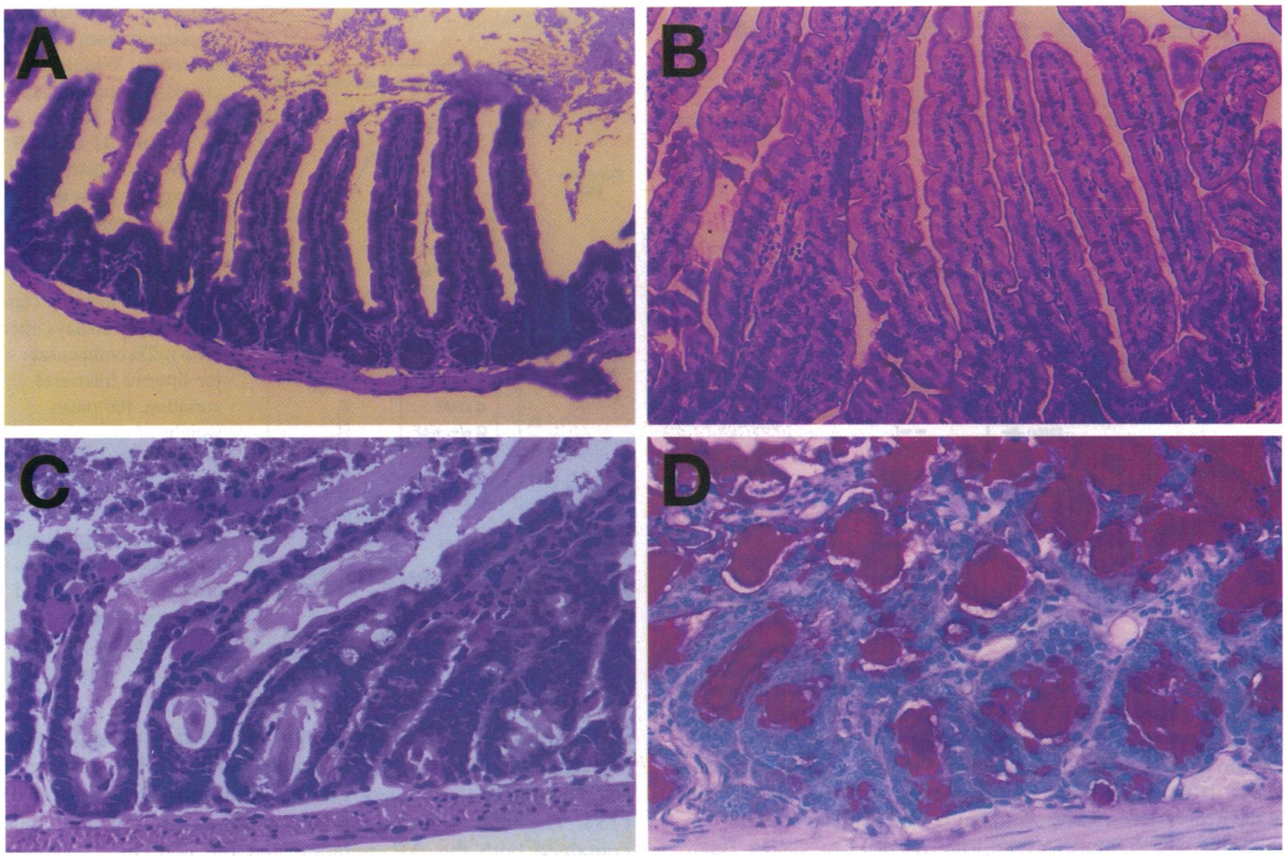

Figure 3. Histological analysis of jejunum from young adult mice (40 d after birth) stained with H&E (A-C) or PAS (D). (A) Jejunum from a +/ΔF animal (200X) showing empty crypts and normal mucosal epithelium. (B) Jejunum from a ΔF/ΔF mouse illustrating essentially normal mucosa (200X). (C) Jejunum from a ΔF/ΔF animal (100X) illustrating abnormal accumulation of mucus. (D) Jejunum from a ΔF/ΔF animal (400X) with mucus accumulation.

Primers were designed to assess the state of RNA spanning CFTR exons 9 and 10 as well as exons 9 and 11. Note that generation of wild-type message between exons 9 and 11 requires correct splicing around the neo^r insertion. Fig. 1 *B* shows that there was no discernible difference in either the size or the quantity of RNA originating from either wild-type (+) or neo^r/neo^r (N) animals. Thus genetic and transcriptional data indicate that the neo^r insertion in intron 10 did not negatively influence expression of the CFTR gene.

Protocols exist that would permit excision of the neo^r marker (29). However they require extended growth and selection of ES cells which could potentially compromise their chimera-forming capacity. Our data suggest that a strategy of cotransfer of a linked marker can be a viable alternative to two-step gene replacement for introducing subtle mutations into mice.

The ΔF mutation reduced the size and viability of mice. The heterozygous progeny of ΔF-containing chimeric mice appeared normal and were fertile. 23 litters from heterozygote (+/ΔF) crosses produced mice with the following genotypes: +/+ = 34 (23%); +/ΔF = 73 (49%); and ΔF/ΔF = 41 (33%). This distribution of offspring is not different from expected values, suggesting that we did not miss perinatal mortality. Shortly after birth, the homozygous ΔF/ΔF offspring manifested two external phenotypes. First, there was an increase in

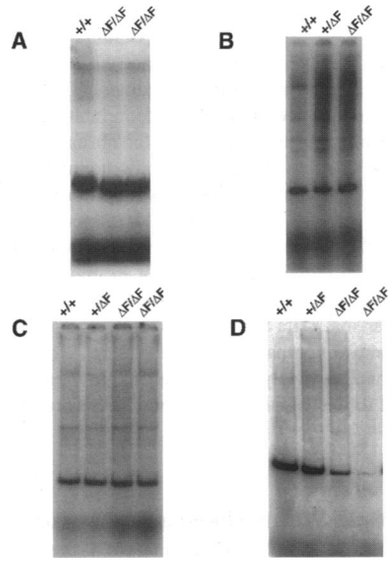

Figure 4. CFTR mRNA from ΔF/ΔF tissue. Total RNA was isolated from testes (A) submaxillary gland (B), lung (C) and upper small bowel (D) from several +/+, +/ΔF and ΔF/ΔF young adult mice and used as substrate for generation of cDNA. Quantitative PCR was performed as described in methods using a single primer set to assay sequences between exons 9 exon 10 (A and D) or exon 10 and 11 (B and C). Product was of predicted size (205 bp and 150 bp, respectively). Genotypes are indicated above each lane.

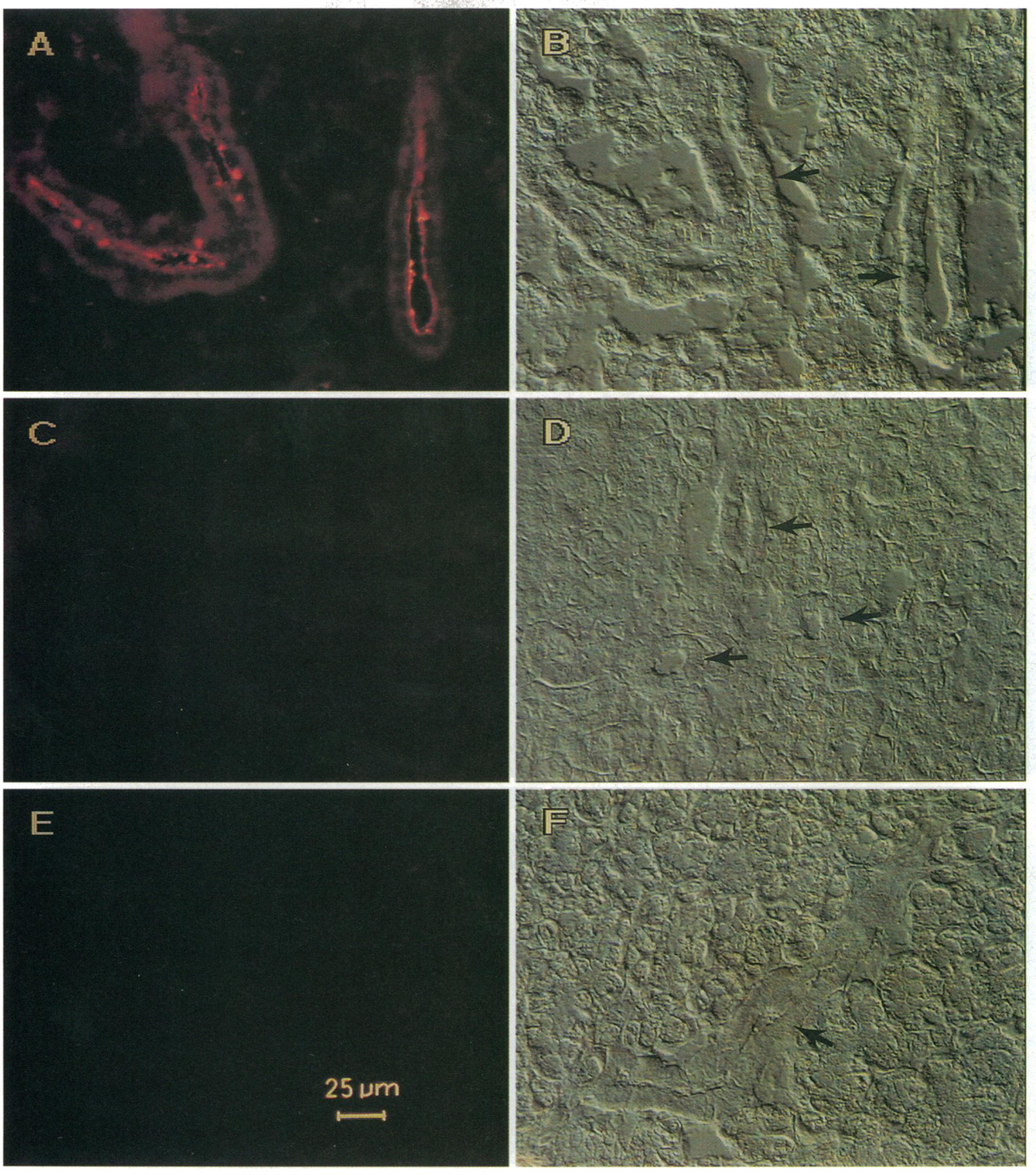

Figure 5. Localization of CFTR in the striated duct of the mouse submaxillary gland. Panels A and B are from a +/+ mouse, panels C and D are from a ΔF/ΔF mouse, and panels E and F are from a CFTR null mouse. Panels A, C, and E show epiflourescent images and panels B, D, and F show the corresponding fields viewed with DIC. Arrows indicate striated ducts in each field.

mortality during the first month after birth (Fig. 2 *A*). Whereas both wild-type (+/+) and heterozygous (+/ΔF) mice suffered < 5% mortality by the time of weaning, ~ 10% of ΔF/ΔF animals died within 7 d of birth. There was significant mortality at the time of weaning (~ 30% days after birth) but ~ 40% of animals survived the postweaning crisis and were viable for at least 8 mo. Second, ΔF/ΔF animals had a marked reduction in size, noticeable as early as 10 d after birth. By the time of weaning, the weight of ΔF/ΔF mice was only 50–60% that of their +/+ and +/ΔF siblings (Fig. 2 *B*). After weaning,

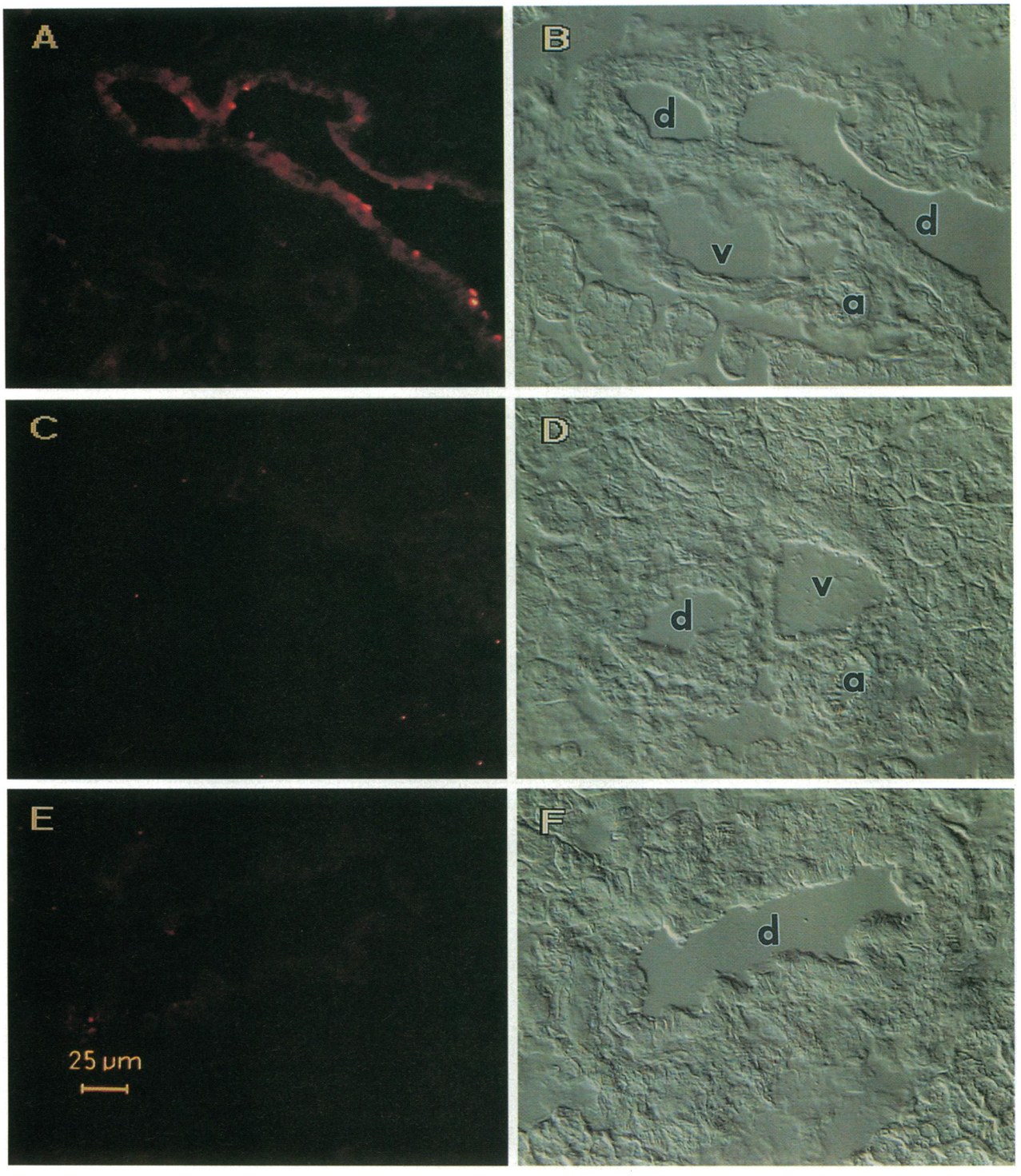

Figure 6. Localization of CFTR in the interlobular duct of the mouse submaxillary gland. Panels are labeled as indicated in Fig. 5. Interlobular ducts and the adjacent arterioles and venules are labeled with the letters "d", "a", and "v", respectively.

ΔF/ΔF animals continued to grow and thrive, though they never achieved the size of their littermates. ΔF/ΔF mice of both sexes were fertile.

Pathology of the gastrointestinal tract and other tissues. Autopsies of animals that died prematurely often showed evidence of peritonitis, bowel obstruction, and bowel strictures (especially in the cecum), but the pathology was highly variable in expressivity. A similar variability in gut pathology was evident in ΔF/ΔF mice killed shortly after weaning. Although tissue isolated from the jejunum of some young adult ΔF/ΔF mice exhibited large casts of mucus material (Fig. 3 *C, D*), tissue from other ΔF/ΔF individuals (Fig. 3 *B*) was indistin-

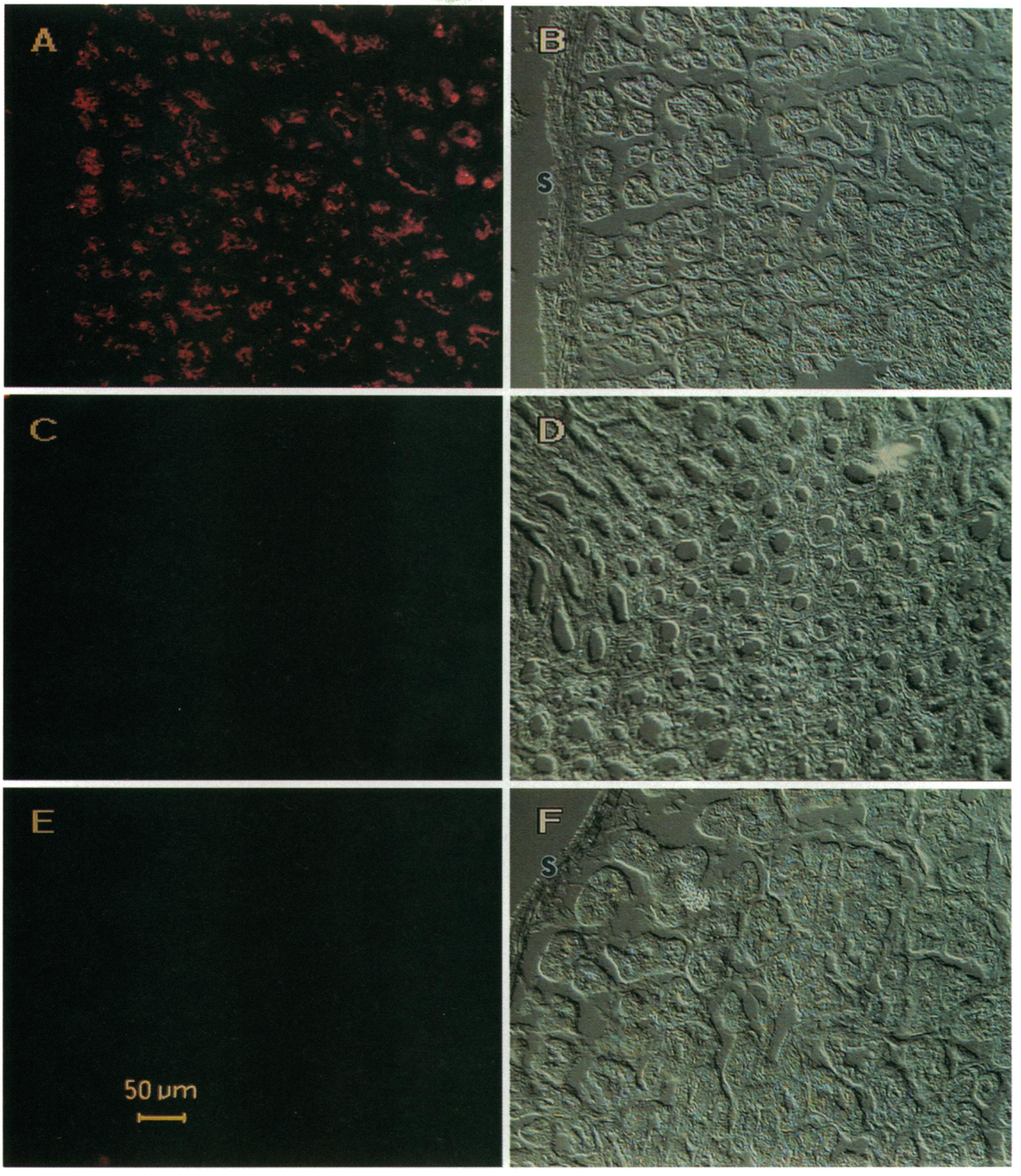

Figure 7. Localization of CFTR in the Brunner's gland of the mouse. Panels are labeled as in Fig. 5. The "s" indicates serosa.

guishable from that of +/ΔF (Fig. 3 *A*) or +/+ mice. These changes are similar to those observed in null mice (9–12).

Analyses of numerous other epithelial and glandular tissues revealed no obvious additional histopathology. Samples of lung, pancreas, gall bladder, male reproductive tract, lacrimal gland, and submandibular glands dissected from four dead and ten killed (and overtly healthy) ΔF/ΔF young adults were all indistinguishable from samples derived from +/+ and +/ΔF animals.

Decreased CFTR transcripts in the intestine of ΔF/ΔF mice. Abnormalities in the intestinal tract of mutant mice were also reflected in the amount of CFTR mRNA which could be isolated from tissue of the upper small bowel. RNA was extracted from duodenum/jejunum, submaxillary glands, lung,

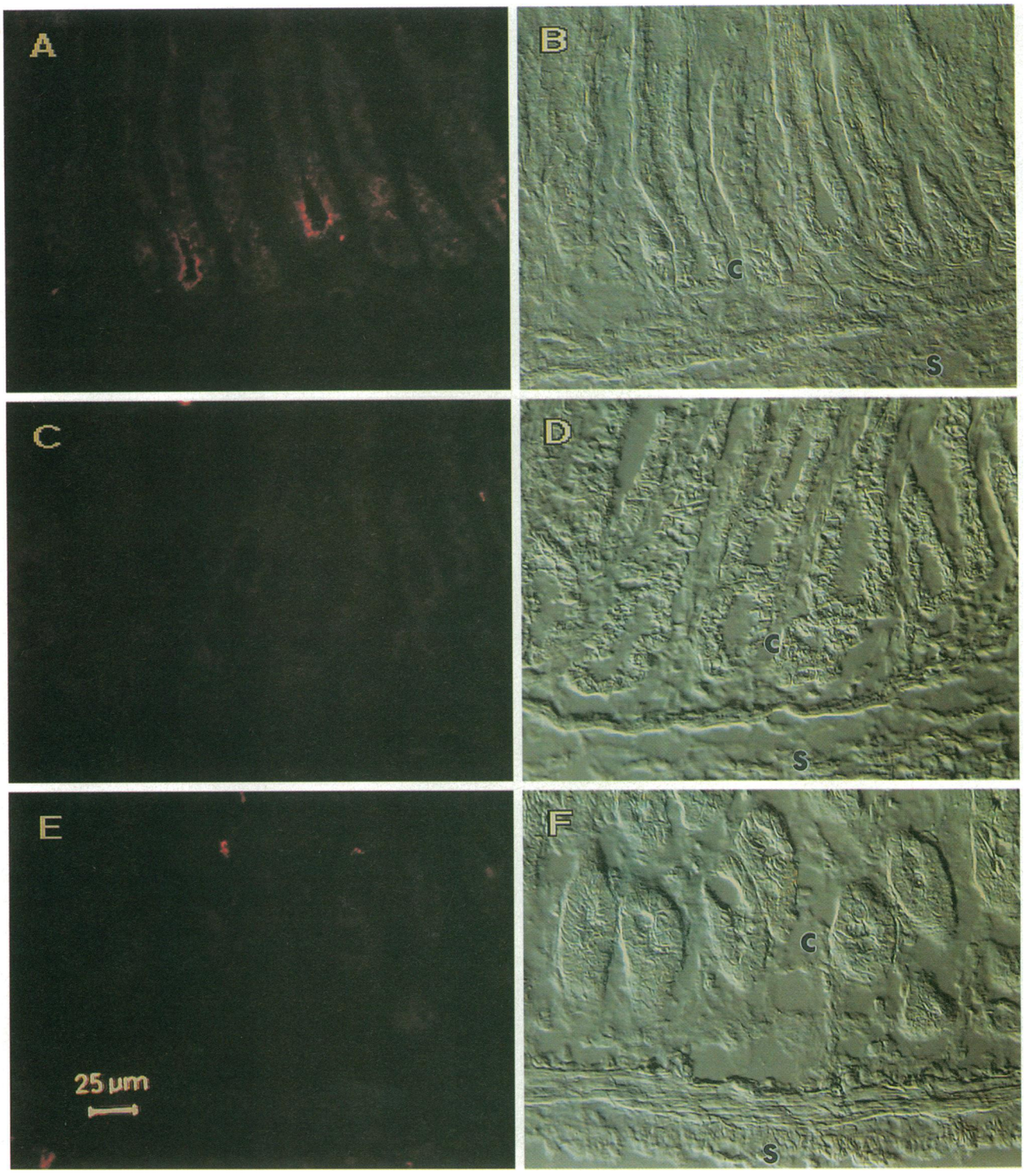

Figure 8. Localization of CFTR in the duodenal crypts of the mouse. Panels are labeled as in Fig. 5. Serosa is labeled with "s" and "c" indicates duodenal crypts.

and testes of healthy young adult male animals and used as substrate for quantitative RT-PCR. Although +/+ and ΔF/ΔF animals had identical amounts of CFTR mRNA derived from testes (Fig. 4 *A*), submaxillary glands (Fig. 4 *B*), and lung (Fig. 4 *C*), the ΔF/ΔF mice showed a marked decrease in the bowel-derived RNA compared to both +/+ and +/ΔF controls (Fig. 4 *D*). Intestine from +/ΔF mice had approximately equal amounts of transcript from the wild-type and the ΔF alleles. Thus loss of CFTR transcripts occurred only in ΔF/ΔF animals and appeared to be tissue specific.

Immunocytochemistry of tissues expressing CFTR. In tissues from humans homozygous for the ΔF508 mutation, CFTR

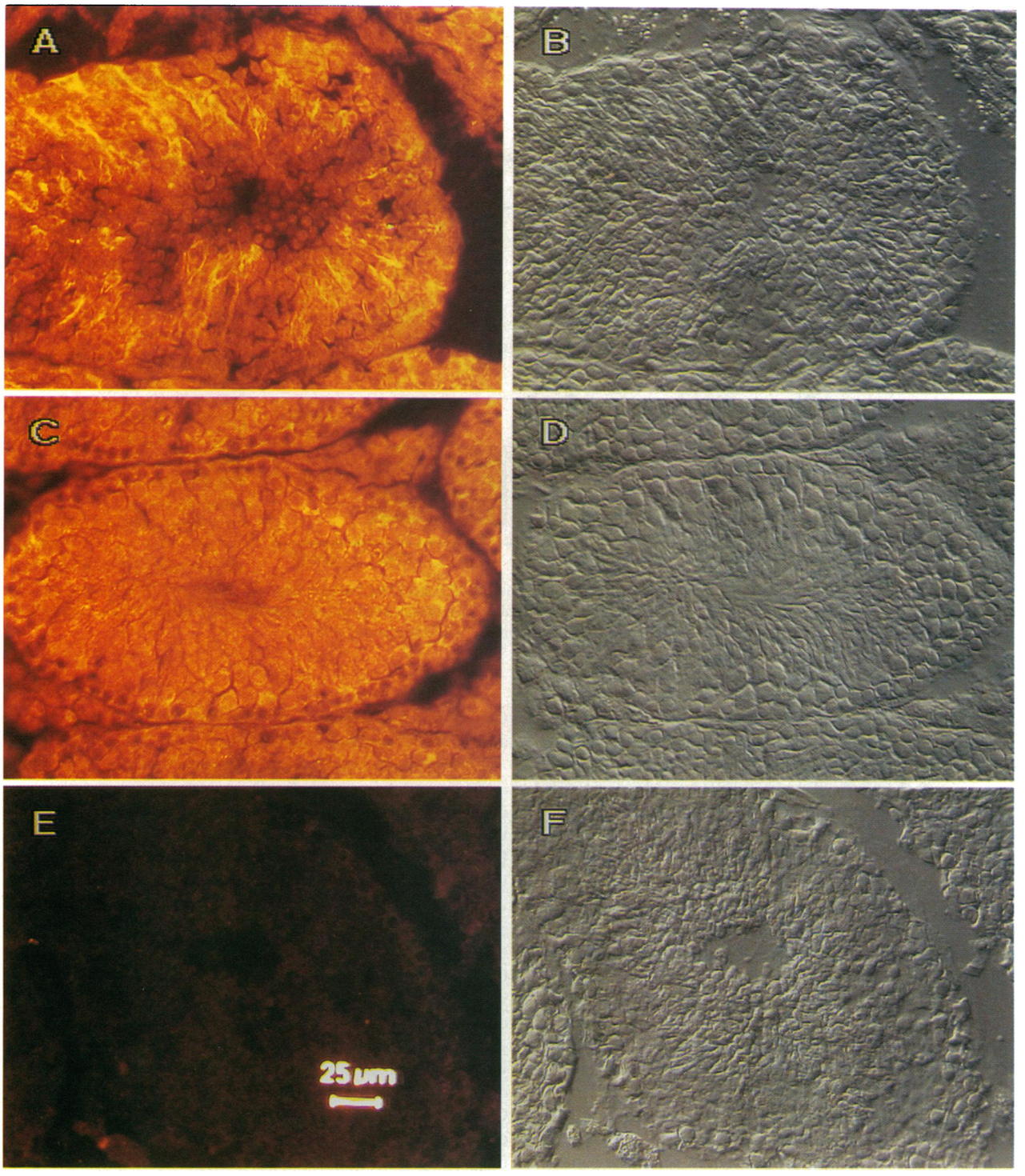

Figure 9. Localization of CFTR in the seminiferous tubules of the mouse testes. Panels are labeled as in Fig. 5.

protein is either not detectable or greatly reduced in amount (5, 6). Therefore, we examined protein distribution in these mice and, as a negative control, in CFTR null mice (11). We observed no specific staining in trachea or pancreas of any of the mice (not shown), a result consistent with previous data indicating that CFTR is expressed at very low levels in these organs in both humans and rodents (5, 30). In submaxillary glands, we found intense apical staining of epithelial cells lining the striated ducts of +/+ (Fig. 5) and +/ΔF mice (not shown). There was also intense staining of a subpopulation of epithelial cells in the interlobular ducts (Fig. 6). In contrast, neither ΔF/ΔF nor null mice showed any specific staining of ducts.

The proximal duodenum of +/+ mice showed marked apical staining of epithelial cells in the Brunner's gland (Fig. 7)

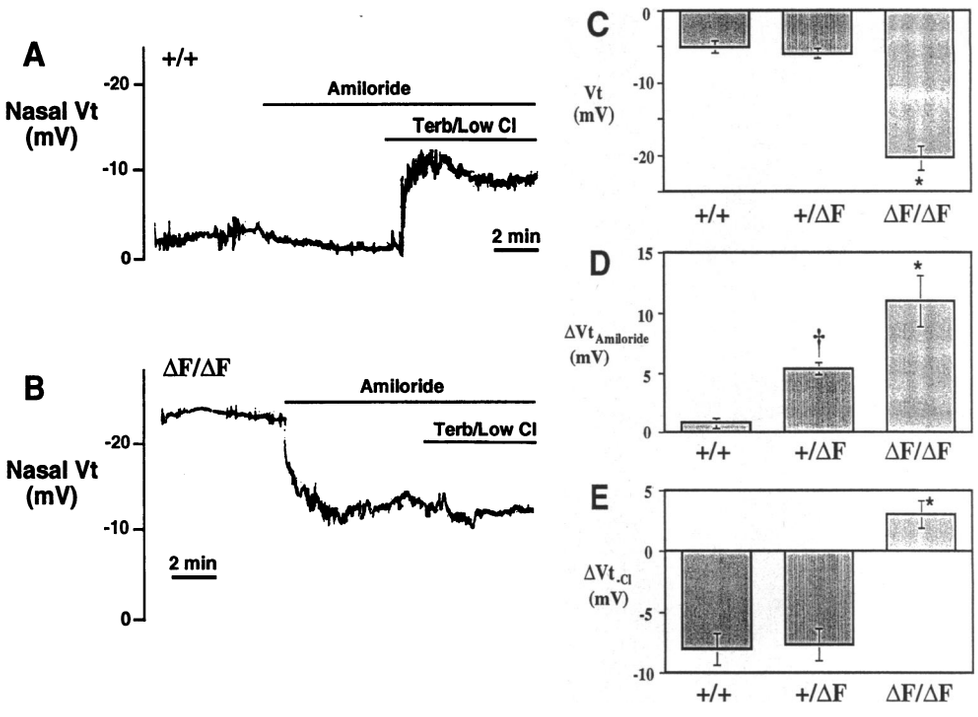

Figure 10. Nasal voltage. Panels A and B show recordings from +/+ and ΔF/ΔF mice, respectively. Bars indicate application of 100 μM amiloride or a solution containing 10 μM terbutaline and a low Cl^- concentration. Panel C shows baseline V_t, panel D shows change in V_t produced by amiloride, and panel E shows change induced by perfusion with terbutaline and a low Cl^- concentration. Data are mean±SEM; n = 9 for +/+ mice, 11 for +/ΔF mice, and 7 for ΔF/ΔF mice. Their mean ages were 42, 39, and 37 days (N.S.) and their mean weights were 18.8, 15.6, and 11.8 g, respectively (N.S.). * indicates $p < 0.001$ compared to +/+ mice. † indicates $p < 0.05$ compared to both +/+ ΔF/ΔF mice. The absolute V_t after addition of amiloride was −2.7±1.2 mV for +/+ mice, −0.9±0.8 mV for +/ΔF mice, and −9.3±3.3 mV for ΔF/ΔF mice. The amiloride-induced change in V_t for +/ΔF animals was intermediate between the +/+ and ΔF/ΔF mice, but because basal V_t and the absolute V_t after addition of amiloride were not different for +/+ and +/ΔF mice, the biological significance of this observation is uncertain. Absolute Vt after addition of amiloride was greater in ΔF/ΔF mice ($p < 0.05$); the reason for this difference was not investigated.

and in the crypts of Lieberkuhn (Fig. 8). CFTR in +/ΔF tissues had a similar localization (not shown). Expression in these tissues agrees with previous studies using in situ hybridization and immunocytochemistry of normal rodent and human tissue (30–32). In ΔF/ΔF and null mice, the Brunner's glands were often dilated (Fig. 7) and they lacked specific staining for CFTR on the apical surface. In the crypts of Lieberkuhn of ΔF/ΔF and null mice, the apical membrane also failed to stain (Fig. 8). Again, the loss of specific staining is consistent with studies of human tissue with the ΔF508 mutation, although we are not aware of any reports on immunocytochemistry of human CF intestine.

We also examined the mouse testes because we detected abundant mRNA expression and because others have detected CFTR mRNA in testes by in situ hybridization (33). We found CFTR expression in all stages of seminiferous tubules. In +/+ and +/ΔF mice, staining appeared to be in the cytoplasm, but also had a striking linear pattern (Fig. 9 *A*). Staining was most prominent in the round spermatids, but was also present in the spermatocytes and elongating spermatids. The linear pattern appeared to represent membrane staining in the regions where round spermatids were closely packed and around the elongating spermatids. Given the limits of our technique, we cannot exclude the possibility that this staining was in part from the sertoli cells. Our immunocytochemical localization is consistent with previous in situ hybridization studies which have shown greatest expression of CFTR mRNA in the round spermatids (33). In ΔF/ΔF mice, specific staining was also present in the cytoplasm, particularly of the round spermatids, but the linear pattern of staining was absent. Testes from CFTR null mice showed no specific staining for CFTR. These data indicate that CFTR protein is present in ΔF/ΔF mice testes; however, it has a different intracellular distribution.

Defective electrolyte and fluid transport in nasal, intestinal, and pancreatic duct epithelia. To evaluate the functional consequences of the ΔF mutation, we studied electrolyte transport in vivo in nasal epithelium by measuring Vt in a blinded fashion. Examples are shown in Fig. 10; *A* and *B* and quantitative data in Fig. 10, *C, D,* and *E.* Under basal conditions, +/+ and +/ΔF mice had a low Vt. When we added amiloride, which blocks apical Na^+ channels, Vt decreased. Then during perfusion with a solution containing the cAMP agonist tebutaline and a low Cl^- concentration Vt hyperpolarized. Hyperpolarization of Vt with this maneuver is due to a diffusion voltage generated through apical CFTR Cl^- channels (25, 26). In contrast, ΔF/ΔF mice had a hyperpolarized basal Vt and a large change with addition of amiloride. Moreover, Vt failed to hyperpolarize during perfusion with terbutaline and solution containing a low Cl^- concentration in any of the ΔF/ΔF mice (the range of change was +1 to +6 mV for ΔF/ΔF mice, compared to a range of −4 to −13 mV for mice in both of the other groups). Thus, ΔF/ΔF mice were distinctly different from +/+ or +/ΔF mice and manifested the same electrophysiologic abnormalities observed in humans with CF (8).

We examined intestinal electrolyte transport in a blinded fashion by testing for the presence of a cAMP-stimulated Cl^- secretory current in freshly excised jejunum mounted in Ussing chambers. The +/+, +/ΔF, and ΔF/ΔF mice all had similar values for basal transepithelial resistance (49.6±5.5, 53.9±3.6, and 39.7±2.6 $\Omega \cdot cm^2$) and basal I_{sc} (12.5±1.7, 9.6±1.7, and 7.3±2.2 $\mu A/cm^2$, respectively). Addition of cAMP agonists caused a prompt increase in I_{sc} in intestine from both +/+ and

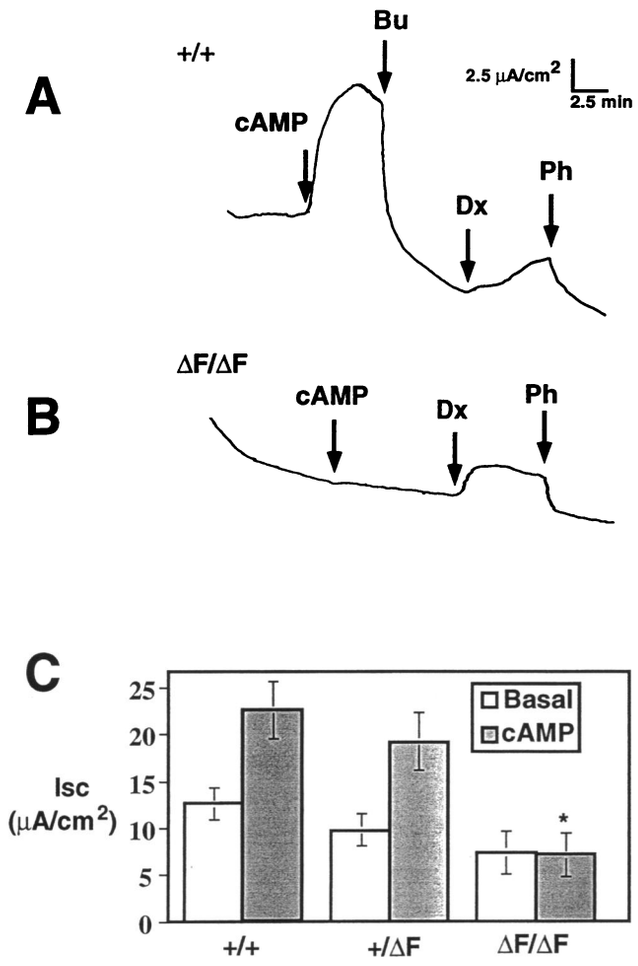

Figure 11. Jejunal short-circuit current, I_{sc}. Panels A and B show representative tracings from +/+ and ΔF/ΔF mice, respectively. cAMP agonists (100 μM IBMX and 10 μM forskolin), 100 μM bumetanide (Bu) were added as indicated by arrows. As an additional test of tissue viability, we added 5 mM dextrose (Dx) and 200 μM phloridzine (Ph) to the mucosal solution to stimulate and inhibit, respectively, electrogenic Na^+-glucose cotransport. Panel C shows average data of basal and cAMP-stimulated currents. There was no significant difference between basal currents in the three groups, but cAMP-stimulated currents were significantly greater in the +/+ and +/ΔF epithelia than in those from ΔF/ΔF mice (*, $p < 0.05$). Data are mean±SEM; n = 9 for +/+ (17 intestinal epithelia), 11 for +/ΔF (20 epithelia), and 7 for ΔF/ΔF (12 epithelia).

+/ΔF mice, but not from ΔF/ΔF mice (Fig. 11). The cAMP-stimulated current was inhibited by the serosal addition of bumetanide, which inhibits Cl^- entry into the cell at the basolateral membrane, confirming that the change was due to Cl^- secretion. The lack of cAMP-stimulated Cl^- secretion in ΔF/ΔF intestine is consistent with abnormalities reported in humans (34–36) and null mice (9–12, 37).

CFTR plays a central role in pancreatic duct secretion, and loss of function causes pancreatic insufficiency in patients with CF (2, 38). Therefore we studied electrolyte transport using pancreatic ducts and ductules cultured on permeable filter supports. Basal I_{sc} and the response to amiloride did not differ between the three groups (Fig. 12 *A*). However, cAMP agonists produced a greater increase in I_{sc} in epithelia from +/+ than from ΔF/ΔF mice. Diphenylamine-2-carboxylate, which inhibits CFTR Cl^- channels (39), inhibited I_{sc} in +/+ and +/ΔF, but not ΔF/ΔF epithelia ($P < 0.001$).

To evaluate the impact of abnormal electrolyte transport on the absorption and secretion of fluid, we measured net fluid transport by cultured pancreatic duct and ductule epithelia (Fig. 12 *B*). Under basal conditions, +/+ and +/ΔF epithelia absorbed fluid, but absorption by ΔF/ΔF epithelia was significantly reduced. cAMP agonists stimulated fluid secretion in epithelia from +/+ mice, whereas ΔF/ΔF epithelia had no change in transport. Interestingly, epithelia from heterozygous +/ΔF animals had a phenotype different from that in +/+ mice in that cAMP agonists produced a smaller change in net fluid transport than was observed in +/+ epithelia.

Discussion

Previous in vitro studies in which the human ΔF508 protein was overexpressed have shown that the mutant protein is retained in the endoplasmic reticulum rather than trafficking to the apical membrane (4). The mutant protein is rapidly degraded and the half-life is shortened (40, 41). As a result, expression of ΔF508 CFTR in most in vitro systems generates little if any Cl^- current. Identification of endogenous ΔF508 CFTR in human tissues has been more difficult because of the low level of expression. Wild-type CFTR can be detected by immunocytochemistry in human bronchial submucosal glands, but in tissue from patients homozygous for the ΔF508 mutation the protein could not be detected, consistent with degradation (6). In the sweat gland duct from patients homozygous for the ΔF508 mutation, the amount of protein was greatly reduced, although some ducts contained what appeared to be cytoplasmic and perinuclear protein (5). Evidence of a cytoplasmic location of mutant protein has also been obtained in nasal polyps (7, 42). This degradation and mislocalization of ΔF protein results in a loss of Cl^- permeability in affected epithelia (2, 8).

Our data suggest that, like human CFTR with the ΔF508 mutation, mouse CFTR-ΔF508 is misprocessed and degraded. In the salivary glands of ΔF/ΔF mice, we were not able to detect ΔF protein, even though the amount of CFTR mRNA was similar to that from +/+ mice. This result suggests that as in humans, the mutant protein is degraded. Additional evidence for mislocalization comes from the testes. In testes from ΔF/ΔF mice CFTR mRNA levels were normal and we detected CFTR protein, but the linear membrane staining observed in +/+ mice was absent. These changes are consistent with our physiologic data which show that epithelia in ΔF/ΔF mice were Cl^- impermeable. Thus the ΔF508 mutation has a similar consequence in mouse and human CFTR.

Mice homozygous for the ΔF508 mutation displayed several phenotypes expected of a severe mutation. The growth retardation, diminished survival, prominent intestinal pathology, and loss of cAMP-stimulated Cl^- transport are features similar to those reported in null mice (9–11, 37). The loss of CFTR activity, as well as the inability to detect apical CFTR in ΔF/ΔF epithelia, argue that the ΔF508 mutation in mice is functionally equivalent to a null allele. Nevertheless, the ΔF homozygotes appeared to be somewhat more robust than the null mice that have been previously described. Approximately 80% of ΔF/ΔF animals survived to weaning compared to 20–

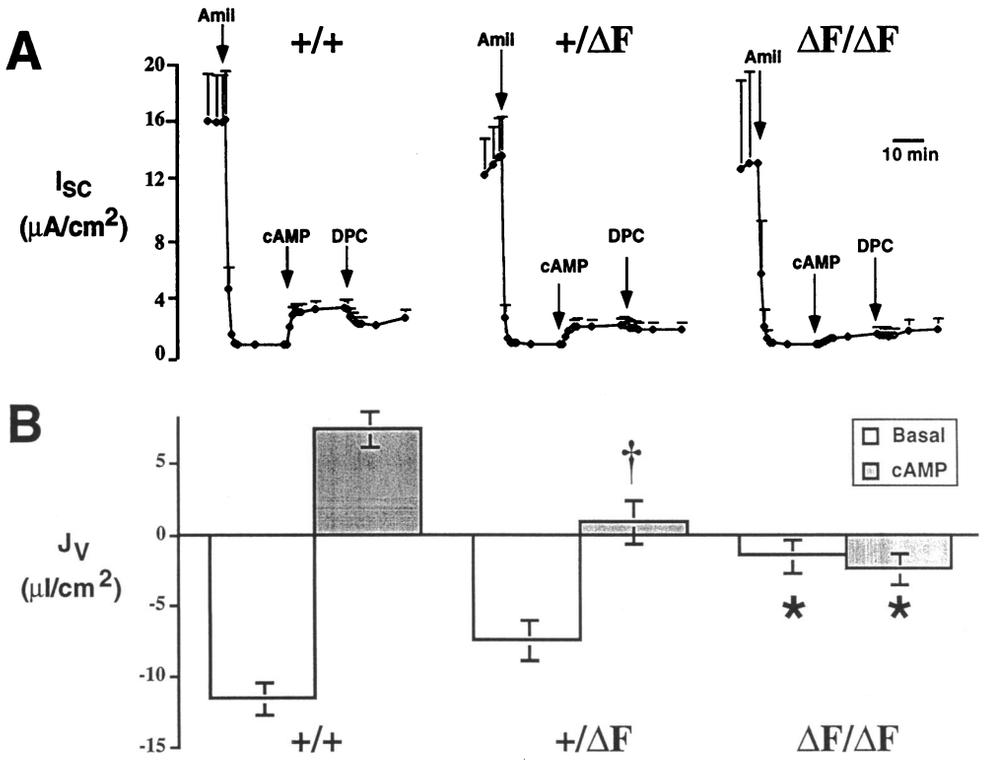

Figure 12. Fluid and electrolyte transport by cultured pancreatic duct epithelia. Panel A shows the I_{sc} data for the +/+, +/ΔF, and ΔF/ΔF mice. The increase in I_{sc} produced by addition of cAMP agonists (100 μM IBMX and 10 μM forskolin) was significantly greater in +/+ than in ΔF/ΔF mice ($p < 0.05$). The cAMP-induced increase in Isc in +/ΔF epithelia was not statistically different from +/+ or ΔF/ΔF epithelia ($p < 0.05$). DPC (2 mM) was added where indicated. n = 12 monolayers from 5 +/+, 6 monolayers from 3 +/ΔF, and 5 monolayers from 2 ΔF/ΔF mice. Transepithelial resistances were 1008, 1160, and 796 Ω·cm², for +/+, +/ΔF, and ΔF/ΔF respectively. Panel B shows net fluid transport measured over 24 hr. Open bars show net transport under basal conditions and shaded bars show transport in presence of cAMP agonists. Negative values indicate net absorption and positive values indicate net secretion. * indicates value significantly different from +/+ mice ($p < 0.001$). † indicates value different from +/+ mice, $p < 0.01$. Data are mean±SEM; n = 68 epithelia from 7 +/+, 76 epithelia from 8 +/ΔF, and 49 epithelia from 5 ΔF/ΔF mice. Transepithelial resistances were 1154, 1325, and 751 Ω·cm², for +/+, +/ΔF, and ΔF/ΔF respectively.

60% perinatal survival reported for null animals (9–11). 40% of ΔF/ΔF mice survived to and thrived in adulthood compared to the 5% reported for homozygous null mice. Factors such as modifier loci (genetic background) and animal husbandry could contribute to differences in survival. However, when null mice were studied with different genetic backgrounds, no appreciable variability in perinatal survival was reported (9, 10). Moreover, the reduced mortality in ΔF/ΔF animals before weaning suggests that a different diet was not responsible. Thus the ΔF508 mutation may be somewhat less severe than the complete disruption of the gene. This result could be explained if a small amount of partially active ΔF protein is delivered to the cell membrane. Because the phenotype of ΔF/ΔF mice was not more severe than that of null mice, these data also indicate that expression of the ΔF508 protein probably has no adverse effect on cell or tissue function.

Study of these mice yielded several other interesting findings. First, we found fewer CFTR transcripts in intestine of ΔF/ΔF animals. There are at least two potential explanations. There may be a tissue-specific down-regulation of CFTR gene transcription in the ΔF/ΔF intestine. Perhaps loss of CFTR function could produce inflammation and inflammatory mediators which activate protein kinase C, resulting in decreased transcription of the CFTR gene (18). Alternatively, there may have been selective loss of CFTR-producing cells and hence a reduction in CFTR transcripts. For example, in humans, loss of CFTR function causes atrophy of the vas deferens and pancreas (2) and presumably decreased mRNA production. Our results in intestine contrast with what we found in submaxillary glands, lung, and testes, where amounts of mRNA were normal. They also contrast with studies in human airway epithelia where quantitative RT-PCR (43) and in situ hybridization (6) suggest that there are normal amounts of CFTRΔF508 transcripts. We are not aware of similar studies in human CF intestine. However, understanding the responsible mechanisms may provide new insight into the regulation of transcription and/or the functional effects of CFTR expression.

A second interesting finding was that the amiloride-sensitive I_{sc} was similar in magnitude in pancreatic epithelia from +/+ and ΔF/ΔF mice. This result contrasts with the greater effect of amiloride on Vt in nasal epithelium of our ΔF/ΔF mice and CFTR null mice (37). It also contrasts with a greater amiloride-sensitive I_{sc} in airway epithelia of humans with CF (44). These data suggest that the presence or absence of CFTR function is not inevitably tied to Na^+ transport. It could be that there is a cell type–specific relationship between CFTR function and Na^+ channel function that is observed in airway but not pancreatic epithelia. Alternatively, airway and pancreatic epithelia might express different amiloride-sensitive Na^+ channels. Comparative study of these tissues may provide a new model to investigate the confusing link between CFTR function and Na^+ transport.

Third, although heterozygous +/ΔF animals resembled +/+ animals in many ways, their pancreatic epithelia showed less cAMP-stimulated fluid secretion than +/+ epithelia. Most electrophysiologic studies have failed to demonstrate an intermediate phenotype in human or mouse heterozygotes. However, the volume of cAMP (β-adrenergic) stimulated fluid secretion by sweat glands of human heterozygotes is half that of normal homozygotes (45, 46). In addition, some but not all reports

suggest that cAMP (cholera toxin) stimulated fluid secretion is decreased in intestine of heterozygous +/null mice (47, 48). Thus, measurement of fluid transport may provide a much more sensitive assay of the absolute amount of functional CFTR in epithelia.

These mice should provide a good model for future research. Approximately 40% of $\Delta F/\Delta F$ mice survive the postweaning crisis, thrive in adulthood, and can live for at least 8 mo. Thus they may prove to be excellent models in which to study the pathogenesis of disease and to examine the effect of various pathogens on the progression of CF lung disease. Like CFTR null mice they can be used to test gene transfer strategies. Finally and most importantly, because they carry the most common CF-associated mutation which appears to have a cellular and tissue defect like that found in humans with the $\Delta F508$ allele, these mice offer the opportunity to test in vivo new strategies for correcting the protein processing and functional defects associated with the $\Delta F508$ mutation.

Acknowledgments

We thank current and past members of the Capecchi and Welsh lab tissue culture and animal core facilities, J. Weis for assistance with RT-PCR, and Phil Karp and Vince Delgadillo for physiologic studies; Drs. John Marshall and Seng Cheng for the gift of the polyclonal antibody, pC-termB; Drs. Wanda O'Neil and Arthur Beaudet for CFTR null mice; and Dr. Frank Longo for reviewing the immunocytochemistry of testes.

This work was supported by the Howard Hughes Medical Institutes (HHMI) and the Cystic Fibrosis Foundation. B. G. Zeiher was supported by a National Heart, Lung, and Blood Institute training grant and J. Zabner by a Parker B. Francis Foundation Fellowship. M. R. Capecchi and M. J. Welsh are Investigators of the HHMI.

References

1. Riordan, J. R., J. M. Rommens, B.-S. Kerem, N. Alon, R. Rozmahel, Z. Grzelczak, J. Zielenski, S. Lok, N. Plavsic, J.-L. Chou, M. L. Drumm, M. C. Iannuzzi, F. S. Collins, and L.-C. Tsui. 1989. Identification of the cystic fibrosis gene: cloning and characterization of complementary DNA. *Science* 245:1066–1073.

2. Welsh, M. J., T. F. Boat, L-C. Tsui, and A. L. Beaudet. 1995. Cystic Fibrosis. *In* The Metabolic Basis of Inherited Disease. C. R. Scriver, A. L. Beaudet, W. S. Sly, and D. Valle, editors. McGraw-Hill, Inc., New York. 3799–3876.

3. Lemma, W. K., G. L. Feldman, B.-S. Kerem, S. D. Fernbach, E. P. Zevkovich, W. E. O'Brien, J. R. Riordan, F. S. Collins, L.-C. Tsui, and A. L. Beaudet. 1990. Mutation analysis for heterozygote detection and the prenatal diagnosis of cystic fibrosis. *N. Engl. J. Med.* 322:291–296.

4. Cheng, S. H., R. J. Gregory, J. Marshall, S. Paul, D. W. Souza, G. A. White, C. R. O'Riordan, and A. E. Smith. 1990. Defective intracellular transport and processing of CFTR is the molecular basis of most cystic fibrosis. *Cell* 63:827–834.

5. Kartner, N., O. Augustinas, T. J. Jensen, A. L. Naismith, and J. R. Riordan. 1992. Mislocalization of delta F508 CFTR in cystic fibrosis sweat gland. *Nature Genet.* 1:321–327.

6. Engelhardt, J. F., J. R. Yankaskas, S. A. Ernst, Y. Yang, C. R. Marino, R. C. Boucher, J. A. Cohn, and J. M. Wilson. 1992. Submucosal glands are the predominant site of CFTR expression in the human bronchus. *Nature Genet.* 2:240–248.

7. Denning, G. M., L. S. Ostedgaard, and M. J. Welsh. 1992. Abnormal localization of cystic fibrosis transmembrane conductance regulator in primary cultures of cystic fibrosis airway epithelia. *J. Cell Biol.* 118:551–559.

8. Knowles, M., J. Gatzy, and R. Boucher. 1983. Relative ion permeability of normal and cystic fibrosis nasal epithelium. *J. Clin. Invest.* 71:1410–1417.

9. Snouwaert, J. N., K. K. Brigman, A. M. Latour, N. N. Malouf, R. C. Boucher, O. Smithies, and B. H. Koller. 1992. An animal model for cystic fibrosis made by gene targeting. *Science* 257:1083–1088.

10. Ratcliff, R., M. J. Evans, A. W. Cuthbert, L. J. MacVinish, D. Foster, J. R. Anderson, and W. H. Colledge. 1993. Production of a severe cystic fibrosis mutations in mice by gene targeting. *Nature Genet.* 4:35–41.

11. O'Neal, W. K., P. Hasty, P. B. McCray, Jr., B. Casey, J. Rivera-Perez, M. J. Welsh, A. L. Beaudet, and A. Bradley. 1993. A severe phenotype in mice with a duplication of exon 3 in the cystic fibrosis locus. *Hum. Mol. Genet.* 2:1561–1569.

12. Dorin, J. R., P. Dickinson, E. W. F. W. Alton, S. N. Smith, D. M. Geddes, B. J. Stevenson, W. L. Kimber, S. Fleming, A. R. Clarke, M. L. Hooper, L. Anderson, R. S. P. Beddington, and D. J. Porteous. 1992. Cystic fibrosis in the mouse by targeted insertional mutagenesis. *Nature* 359:211–215.

13. Deng, C., K. R. Thomas, and M. R. Capecchi. 1993. Location of crossovers during gene targeting with insertion and replacement vectors. *Mol. Cell. Biol.* 13:2134–2140.

14. Tata, F., P. Stanier, C. Wicking, S. Halford, H. Kruyer, N. J. Lench, P. J. Scambler, C. Hansen, J. C. Braman, R. Williamson, and B. J. Wainwright. 1991. Cloning the mouse homolog of the human cystic fibrosis transmembrane conductance regulator gene. *Genomics* 10:301–307.

15. Yorifuji, T. 1991. Molecular cloning and sequence analysis of the murine cDNA for the cystic fibrosis transmembrane conductance regulator. *Genomics* 10:547–550.

16. Denning, G. M., M. P. Anderson, J. Amara, J. Marshall, A. E. Smith, and M. J. Welsh. 1992. Processing of mutant cystic fibrosis transmembrane conductance regulator is temperature-sensitive. *Nature* 358:761–764.

17. Dalemans, W., P. Barbry, G. Champigny, S. Jallat, K. Dott, D. Dreyer, R. G. Crystal, A. Pavirani, J. P. Lecocq, and M. Lazdunski. 1991. Altered chloride ion channel kinetics associated with the $\Delta F508$ cystic fibrosis mutation. *Nature* 354:526–528.

18. Chu, C. S., B. C. Trapnell, J. J. J. Murtagh, J. Moss, W. Dalemans, S. Jallat, A. Mercenier, A. Pavirani, J.-P. Lecocq, G. R. Cutting, W. B. Guggino, and R. G. Crystal. 1992. Cystic fibrosis transmembrane conductance regulator (CFTR) gene transcripts. *EMBO J.* 11:379–380.

19. Robertson, E., A. Bradley, M. Kuehn, and M. Evans. 1986. Germ-line transmission of genes introduced into cultured pluripotential cells by retroviral vectors. *Nature* 323:445–447.

20. Thomas, K. R. and M. R. Capecchi. 1990. Targeted disruption of the murine *int*-1 proto-oncogene resulting in severe abnormalities in midbrain and cerebellar development. *Nature* 346:847–850.

21. Thomas, K. R. and M. R. Capecchi. 1987. Site-directed mutagenesis by gene targeting in mouse embryo-derived stem cells. *Cell* 51:503–512.

22. Cathala, G., J.-F. Savouret, B. Mendez, B. L. West, M. Karin, J. A. Martial, and J. D. Baxter. 1983. A method for isolation of intact, translationally active ribonucleic acid. *DNA* 2:329–335.

23. Tan, S. S. and J. H. Weis. 1992. Development of a sensitive reverse transcriptase PCR assay, RT-RPCR, utilizing rapid cycle times. *PCR Methods Appl.* 2:137–143.

24. Mansour, S. L., J. M. Goddard, and M. R. Capecchi. 1993. Mice homozygous for a targeted disruption of the proto-oncogene *int*-2 have developmental defects in the tail and inner ear. *Development* 117:13–28.

25. Knowles, M. R., L. L. Clarke, and R. C. Boucher. 1991. Activation by extracellular nucleotides of chloride secretion in the airway epithelia of patients with cystic fibrosis. *N. Engl. J. Med.* 325:533–538.

26. Alton, E. W. F. W., D. Currie, R. Logan-Sinclair, J. O. Warner, M. E. Hodson, and D. M. Geddes. 1990. Nasal potential difference: a clinical diagnostic test for cystic fibrosis. *Eur. Respir. J.* 3:922–926.

27. Githens, S., J. A. Schexnayder, R. L. Moses, G. M. Denning, J. J. Smith, and M. L. Frazier. 1994. Mouse pancreatic acinar/ductular tissue gives rise to epithelial cultures that are morphologically, biochemically, and functionally indistinguishable from interlobular duct cell cultures. *In Vitro Cell. Dev. Biol.* 30A:622–635.

28. Smith, J. J. and M. J. Welsh. 1993. Fluid and electrolyte transport by cultured human airway epithelia. *J. Clin. Invest.* 91:1590–1597.

29. Ramirez-Solis, R., H. Zheng, J. Whiting, R. Krumlauf, and A. Bradley. 1993. *Hoxb-4* (*Hox-2.6*) mutant mice show homeotic transformation of a cervical vertebra and defects in the closure of the sternal rudiments. *Cell* 73:279–294.

30. Trezise, A. E. and M. Buchwald. 1991. *In vivo* cell-specific expression of the cystic fibrosis transmembrane conductance regulator. *Nature* 353:434–437.

31. Strong, T. V., K. Boehm, and F. S. Collins. 1994. Localization of cystic fibrosis transmembrane conductance regulator mRNA in the human gastrointestinal tract by *in situ* hybridization. *J. Clin. Invest.* 93:347–354.

32. Gaillard, D., S. Ruocco, A. Lallemand, W. Dalemans, J. Hinnrasky, and E. Puchelle. 1994. Immunohistochemical localization of cystic fibrosis transmembrane conductance regulator in human fetal and airway and digestive mucosa. *Pediatr. Res.* 36:137–143.

33. Trezise, A. E., C. C. Linder, D. Greiger. E. W. Thompson, H. Meunier, J. D. Griswold, and M. Buchwald. 1993. CFTR expression is regulated during both the cycle of the semiferous epithelium and the oestrous cycle of rodents. *Nature Genet.* 3:157–164.

34. Veeze, H. J., M. Sinaasappel, J. Bijman, J. Bouquet, and H. R. De Jonge. 1991. Ion transport abnormalities in rectal suction biopsies from children with cystic fibrosis. *Gastroenterology* 101:398–403.

35. Berschneider, H. M., M. R. Knowles, R. G. Azizkhan, R. C. Boucher, N. A. Tobey, R. C. Orlando, and D. W. Powell. 1988. Altered intestinal chloride transport in cystic fibrosis. *FASEB J.* 2:2625–2629.

36. Goldstein, J. L., A. B. Shapiro, M. D. Rao, and T. J. Layden. 1991. *In vivo* evidence of altered chloride but not potassium secretion in cystic fibrosis rectal mucosa. *Gastroenterology* 101:1012–1019.

37. Clarke, L. L., B. R. Grubb, S. E. Gabriel, O. Smithies, B. H. Koller, and R. C. Boucher. 1992. Defective epithelial chloride transport in a gene-targeted mouse model of cystic fibrosis. *Science* 257:1125–1130.

38. Marino, C. R., L. M. Matovcik, F. S. Gorelick, and J. A. Cohn. 1991. Localization of the cystic fibrosis transmembrane conductance regulator in pancreas. *J. Clin. Invest.* 88:712–716.

39. McCarty, N. A., S. McDonough, B. N. Cohen, J. R. Riordan, N. Davidson, and H. A. Lester. 1993. Voltage-dependent block of the cystic fibrosis transmembrane conductance regulator Cl-channel by two closely related arylaminobenzoates. *J. Gen. Physiol.* 102:1–23.

40. Lukacs, G. L., X.-B. Chang, C. Bear, N. Kartner, A. Mohamed. J. R. Riordan, and S. Grinstein. 1993. The ΔF508 mutation decreases the stability of cystic fibrosis transmembrane conductance regulator in the plasma membrane. Determination of functional half-lives on transfected cells. *J. Biol. Chem.* 268:21592–21598.

41. Ward, C. L. and R. R. Kopito. 1994. Intracellular turnover of cystic fibrosis transmembrane conductance regulator: Inefficient processing and rapid degradation of wild-type and mutant proteins. *J. Biol. Chem.* 269:25710–25718.

42. Puchelle, E., D. Gaillard, D. Ploton, J. Hinnrasky, C. Fuchey, M.-C. Boutterin, J. Jacquot, D. Deyer, A. Pavirani, and W. Dalemans. 1992. Differential localization of the cystic fibrosis transmembrane conductance regulator in normal and cystic fibrosis airway epithelium. *Am. J. Respir. Cell Mol. Biol.* 7:485–491.

43. Trapnell, B. C., C. S. Chu, P. K. Paakko, T. C. Banks, K. Yoshimura, V. J. Ferrans, M. S. Chernick, and R. G. Crystal. 1991. Expression of the cystic fibrosis transmembrane conductance regulator gene in the respiratory tract of normal individuals and individuals with cystic fibrosis. *Proc. Natl. Acad. Sci. USA* 88:6565–6569.

44. Boucher, R. C., M. J. Stutts, M. R. Knowles, L. Cantley, and J. T. Gatzy. 1986. Na+ transport in cystic fibrosis respiratory epithelia. Abnormal basal rate and response to adenylate cyclase activation. *J. Clin. Invest.* 78:1245–1252.

45. Behm, J. K., G. Hagiwara, N. J. Lewiston, P. M. Quinton, and J. J. Wine. 1987. Hyposecretion of beta-adrenergically induced sweating in cystic fibrosis heterozygotes. *Pediatr. Res.* 22:271–276.

46. Sato, K. and F. Sato. 1988. Variable reduction in beta-adrenergic sweat secretion in cystic fibrosis heterozygotes. *J. Lab. Clin. Med.* 111:511–518.

47. Gabriel, S. E., K. N. Brigman, B. H. Koller, R. C. Boucher, and M. J. Stutts. 1994. Cystic fibrosis heterozygote resistance to cholera toxin in the cystic fibrosis mouse model. *Science* 266:107–109.

48. Cuthbert, A. W., J. Halstead, R. Ratcliff, W. H. Colledge, and M. J. Evans. 1995. The genetic advantage hypothesis in cystic fibrosis heterozygotes: a murine study. *J. Physiol.* 482.2:449–454.